Electric Field Enhanced Adsorption and Diffusion of Adatoms in MoS_2 Monolayer

Wenwu Shi,[1] Zhiguo Wang,[1*] Zhijie Li,[1] Y.Q. Fu[1,2*]

1 *School of Physical Electronics, Center for Public Security Information and Equipment Integration Technology, University of Electronic Science and Technology of China, Chengdu, 610054, P.R. China*
2 *Faculty of Engineering and Environment, University of Northumbria, Newcastle upon Tyne, NE1 8ST, UK*

[*]Corresponding author. E-mail: zgwang@uestc.edu.cn (ZW); richard.fu@northumbria.ac.uk (YF)

Abstract:

A new phenomenon, electric field enhanced adsorption and diffusion of lithium, magnesium and aluminum ions in a MoS_2 monolayer, was investigated using density functional theory in this study. With the electric field increased from 0 to 0.8 V/Å, the adsorption energies of the Li, Mg and Al atoms in the MoS_2 monolayer were decreased from -2.01 to -2.49 eV, from -0.80 to -1.28 eV, and -2.71 to -3.01 eV, respectively. The corresponding diffusion barriers were simultaneously decreased from 0.23 to 0.08 eV, from 0.15 to 0.10 eV, and 0.24 to 0.21 eV for the Li, Mg and Al ions, respectively. We concluded that the external electric field can increase the charging speed of rechargeable ion batteries based on the MoS_2 anode materials.

Keywords：monolayers; ab initio calculations; diffusion; adsorption

1. Introduction

Layered structural materials are convenient for intercalation/deintercalation of metal ions, thus can be used as the appropriate materials for rechargeable ion batteries [1-4]. Among them, graphite is the key anode material for the commercial lithium ion batteries (LIBs) with an energy capacity of 372 $mAhg^{-1}$ [5]. The electrochemical performance of the LIBs can be improved by reducing the size of electrode materials [6-8]. Reducing the thickness of the graphite can significantly improve its energy capacity, and a mono-layer of graphene has much higher energy capacities of 600-1000 mAh/g [9, 10]. Other types of monolayer materials such as molybdenum disulfide (MoS_2) [11], V_2O_5 [12], and transition-metal nitride [13] have also received much attention to be used as the electrode materials for the LIBs. Recently, MoS_2 with a graphite-like layered structure has been explored as a new generation of renewable energy related materials, used as catalysts for dissociation of H_2O [14], catalysts for hydrogen evolution reaction [15], and anode materials for the rechargeable ion batteries [16-18]. Monolayer of the MoS_2 has been synthesized using various methods, such as scotch tape based micromechanical exfoliation [19, 20], molybdenum oxide sulfurization [21, 22], and physical vapor deposition [23]. Furthermore, MoS_2/graphene nanocomposites have been used as an anode for the LIBs and the device exhibited a high specific capacity of 1225-1400 mAh/g [24, 25]. After 200 repeated charge-discharge cycles, it still maintained a high value of 1351 mA h/g [26].

Currently the energy density and cycle life of the LIBs cannot meet the critical requirement of electric vehicles and renewable energy storage, also the resource of lithium is insufficient for future use. Therefore, it is essential to search and develop new types of transporting ions which are cheaper and environmentally friendly for the rechargeable ion batteries with large energy/power densities. Sodium and magnesium are abundant on the earth, which could provide

solutions as the new types of rechargeable ion batteries with a low cost and safe energy storage [27, 28]. Experimental and theoretical work has already been performed to apply the MoS_2 nano-layers as the anode materials for the LIBs, sodium ion batteries and magnesium ion batteries [29-36].

Practically, an ideal anode material should have a low diffusion barrier for the transporting ions in order to achieve a fast charging rate. At the same time, the anode materials should have a large exothermic reaction energy for the transporting ions in order to achieve a large storage capacity [37]. The diffusion barriers for the Li and Na in a monolayer of MoS_2 calculated using density function theory (DFT) are 0.24 [38] and 0.68 eV [34] , respectively, and the Li mobility can be enhanced using the MoS_2 nanoribbons by reducing the dimensions [39]. Defects including single- and few-atom vacancies, antisite, and grain boundary are inevitable, thus the effects of defects on the electronic properties of the MoS_2 have been investigated [40, 41]. A recent study showed that these defects can enhance the exothermic reaction of Li adsorption in the MoS_2 monolayer [42].

It is well-known that the external electric field can be used to modify the physical properties of nanomaterials such as SiC nanotubes [43], MoS_2 monolayers [44] and nanoribbons [45]. Application of the electrical field into the nano-materials is practically achievable because of its easily controllable direction and intensity. For example, the adsorption of gas molecules on a monolayer MoS_2 has been investigated by considering the external electric field [46]. In this work, we investigated the effects of an external electric field on adsorption and diffusion of Li/Mg/Al ions in the MoS_2 monolayer based on DFT analysis. The reason why we choose the Li, Mg and Al ions for the study is to represent those common ions in the mono-, bi- and tri-valent rechargeable ion batteries. We have reported, for the first time, that adsorption and mobility of

the transporting ions can be significantly enhanced in the MoS_2 monolayer with an external electric field. Based on the results, we proposed a new design for the next generation of fast charging rechargeable ion batteries.

2. SIMULATION DETAILS

Adsorption and diffusion of the transporting ions in the MoS_2 monolayer were calculated using DFT code of SIESTA [47], in which the core electrons and valence electrons were described using nonlocal norm-conserving pseudo-potentials and a linear combination of numerical pseudo-atomic orbitals [48]. The valence electron wave functions were expanded using double-ζ basis set plus polarization functions. The generalized gradient approximation (GGA) [49] was used to describe the electron exchange-correlation functional. An energy mesh cutoff of 200 Ry was used for the self-consistent Hamiltonian matrix elements when the charge density was projected on a real space grid.

For the MoS_2 monolayer, a 5×5 hexagonal supercell model containing 50 S atoms and 25 Mo atoms plus one Li/Mg/Al ion was used for all the simulations. In order to avoid the periodic image interactions between the MoS_2 monolayers, the distance between the two adjacent layers was kept as 25 Å. A special *k*-point sampling with 3×3×1 *k*-grid was performed for the Brillouin zone integration of the Monkhorst-Pack scheme [50]. As mentioned before, Li, Mg and Al elements were investigated as the transporting ions for the rechargeable ion batteries.

The adsorption energy (E_{ads}) which indicates the interactions between transporting ions and MoS_2 monolayer was calculated using equation (2).

$$E_{ads} = E_{MoS_2-M} - E_{MoS_2} - E_M \quad (2)$$

where E_{MoS_2-M} and E_{MoS_2} are the total energies of the MoS_2 with and without adsorption of the transporting ions, respectively, and E_M is the energy of an isolated transporting atom. The more negative value of the adsorption energy is, the more favorable exothermic reactions could occur between the monolayer MoS_2 and transporting ions.

The adsorption and diffusion behaviors were investigated under an external electric field, which was applied in the direction perpendicular to the MoS_2 monolayer as shown in Fig. 1(b), and the electric field intensity was set from 0.0 V/Å to 0.8 V/Å with its step increment set as 0.1 V/Å. Our tests have shown that the direction of electrical field perpendicular to the MoS_2 monolayer has more significant effect on the reduction of energies barriers than the other directions. The electric field was featured as an additional saw-tooth potential profile perpendicular to the monolayer MoS_2 as described in Reference [51].

3. RESULTS AND DISCUSSION

Adsorption of atoms on the MoS_2 monolayer has been studied in literature [39, 52]. There are two dominant adsorption sites for the atoms, i.e., ST (top of the S atom) site, T (top of the molybdenum) site and H (center of the hexagon) site as shown in Fig. 1. T site is the energy favorable one among these three sites for all the Li, Mg and Al atoms. For example, the calculated adsorption energy for the Li adsorption on a pristine MoS_2 monolayer at the T site is -2.01 eV with a Li-S bond length of 2.40 Å. The T site has an adsorption energy which is 120 meV energetically lower for the Li adsorption compared with that at the H site, which agrees well with the literature [53]. The adsorption energy for the Mg in the MoS_2 monolayer is -0.80 eV per Mg atom, which agrees with the previously reported value of -0.70 eV [54]. The adsorption energies are -2.53 and -2.71 eV for the Al adsorbed at the H and T sites, respectively.

The changes of the adsorption energies at different electric fields for the Li, Mg and Al adsorbed on the MoS_2 monolayer are shown in Fig. 2. When the external electric field is increased from 0.0 to 0.8 V/Å, the adsorption energies decrease from -2.01 to -2.49 eV, from -0.80 to -1.28 eV, and from -2.71 to -3.01 eV for the Li, Mg and Al atoms adsorbed at H sites, respectively. Results clearly show that the external electric field enhances the exothermic reactions between the monolayer MoS_2 and Li/Mg/Al atoms. The energy density is determined by the reversible capacity and operating voltage, which are determined by the chemistry of the electrode material, i.e., its effective redox couples and maximum lithium concentrations [55]. The large exothermic reaction energy between the Li, Mg and Al and MoS_2 monolayer indicates that the anode materials have a large energy storage capacity.

Several methods, including Nudged Elastic Band (NEB) method, dimer method, and constrained method, can be used to determine the diffusion barriers of the condensed matters [56]. The constrained method is the simplest but also the most intuitive one among the different methods. As the NEB method has not been included into the main SIESTA code, in this study the diffusion barriers were calculated using a constrained method in the present work, in which the ions were constrained in the direction along the diffusion path, whereas it is allowed to relax in the direction perpendicular to the diffusion path. The diffusion path for the Li, Mg and Al atoms in the MoS_2 monolayer is from a T site to another nearest T site by passing through the metastable H site [38] as shown in Fig. 3 (a). The energy barrier curves for the Li, Mg and Al diffusion without and with the electric fields are shown in Figs. 3(b) to 3(d), respectively. The diffusion barriers calculated using the constrained methods agree well with the values calculated using an NEB method [57]. For example, the diffusion barrier of the Li in the pristine MoS_2 monolayer is 0.23 eV, which agrees well with the previously calculated results of 0.21 [53] and

0.24 eV using the NEB methods [38]. The calculated diffusion barrier for the Mg in the MoS_2 monolayer is 0.15 eV without applying an electric field. The previously reported values are 0.08 eV for the Mg in MoS_2 monolayer [54] and 0.22 eV in bi-layered MoS_2 with increasing the interlayer spacing up to 0.9 nm [29].

The diffusion energy barriers as a function of electric field as the Li, Mg and Al diffuse on the MoS_2 monolayer are shown in Fig. 4. It is interesting to find that the diffusion barriers decrease significantly after applying the external electric field, and the values for the Li atoms in the MoS_2 layer are 0.23, 0.17, 0.13 and 0.09 eV with external electric fields of 0.0, 0.3, 0.5 and 0.7 V/Å, respectively. The decrease of diffusion barriers shows an apparent dependence on the valence of cations, and this decreasing trend is more obvious for the monovalent Li than those for the divalent Mg and trivalent Al. The diffusion barriers decrease from 0.23 to 0.08 eV, from 0.15 to 0.10 eV, and from 0.24 to 0.21 eV for the Li, Mg and Al atoms, respectively, as the electric field is increased from 0.0 to 0.8 V/Å. The difference is associated to the smaller polarizing strength of the Li ions compared with those of the Mg and Al ions [29].

The diffusion coefficient varies exponentially with the diffusion barrier following an Arrhenius-like formula [58]: $D \propto e^{-E_A/k_BT}$, where E_A is the diffusion barrier, k_B the Boltzmann constant and T the temperature. Therefore, the reduction of energy barrier of 0.06 eV could change the ion mobility by a factor of ~10 at room temperature. The decreases of energy barriers for the Mg and Al ions are smaller than that for Li ion. Therefore, the effect of electric field is much more effective for the LIBs. The diffusion coefficient of the Li can be improved 10 and 100 times by applying 0.3 and 0.6 V/Å, respectively.

Previous study showed that the van der Waals (vdW) interactions have a significant impact on both binding energies of metal and hydrogen on graphene [59]. The vdW interactions can

stabilize the inserted ions and hinder ion diffusion in a layered V_2O_5 [60]. To assess the role of vdW interactions in the diffusion on the MoS_2 with an electrical field, we also considered the vdW interactions proposed by Dion et al. [61]. The obtained diffusion profiles are shown in Fig. 4b. The diffusion barriers are 0.22, 0.19 and 0.16 eV with external electric fields of 0.0, 0.3, and 0.5 V/Å, respectively. The diffusion barriers are decreased by adding the external electrical field with the considering of the vdW interactions.

Effect of the electrical field on the diffusion of Li with a large concentration of Li was investigated, and the results are shown in Fig. 5 (a). Four Li atoms were adsorbed on the same super cell as used above. The energy diffusion profiles are shown in Fig. 5(b). It can be seen that the diffusion barriers are 0.28 and 0.21 eV with external electric fields of 0.0 and 0.3 V/Å, respectively. The diffusion barriers were decreased after applying the electric field for high concentration of the Li.

Adsorption energies and diffusion barriers are two important parameters to characterize the electrochemical performance of the anode materials. Large negative values of the adsorption energies indicate that the anode materials have a large energy storage capacity [37]. Small values of the diffusion barriers indicate that the anode can be charged with a fast charging rate. It was reported that certain defects formed in materials of graphene [37, 62-65] and silicone [66] can enhance the adsorption of lithium in these materials. Although the diffusion barriers of lithium from pristine to the defects site in the MoS_2 monolayer have been reduced, the reverse diffusion barriers have actually been increased. Because the defects are the trapping centers for the lithium atoms, therefore, if these lithium atoms have been adsorbed into these sites, they could not participate in the following electrochemical process.

Our simulation results clearly showed that the external electric field can enhance the adsorption of the Li, Mg and Al atoms onto the MoS_2 monolayer, and simultaneously decrease the diffusion barrier. Based on the simulation results, we proposed a new structure of charging process for the rechargeable ion batteries as schematically shown in Fig. 6. The charging process is same with that of a conventional charger, except for the additional power supply enclosed by the dotted line as shown in Fig. 6, which can provide an electrical field on the anode material after switched on. The batteries behave as a conventional battery when switched off. When the batteries are charged, the electric field can be applied to the anode materials. As the electric field can enhance the exothermic reactions between the transporting ions and anode materials, the larger the electric field is, the more exothermic reactions occur. Also the diffusion barriers can be decreased by the presence of the electric field, thus the setup can be used to accelerate the charging process. The batteries function as a normal unit to supply the output power if the external electrical filed is switched off. It should be notified that the above results of enhancement of adsorption and diffusion by external electrical field were obtained from the analysis based on a monolayer of MoS_2. As the Li is sited above ~2 Å above the monolayer, the interlayer distance should be larger than 4.0 Å as shown in Fig. 6, in order to make the electrical field more effective.

From the above results, an external electric field can enhance the adsorption and diffusion of the Li/Mg/Al ions in the MoS_2 monolayer based on the DFT analysis, which provides a novel route for the fast charging process. As the Li/Mg/Al atoms are adsorbed on the MoS_2, charge transfer from the atoms to the MoS_2 occurs [42, 67]. The amount of charge transferred from the atoms will increase with the increase of strength of the electric field, and the difference in the charge transfer at the different sites will decrease with increasing strength of the electric field.

Therefore, the adsorption will be enhanced and the diffusion energy barriers will be decreased with increasing the electric field. The enhancement mechanisms of the adsorption and diffusion can also be used in other anode materials, such as graphene, carbon nanotubes and black phosphorus.

4. CONCLUSION

In conclusion, the adsorption and diffusion behaviors of the Li, Mg and Al atoms on MoS_2 monolayer with an external electric field were investigated using the DFT method. The electric field enhanced the exothermic reaction between the monolayer MoS_2 and atoms. Meanwhile, the diffusion barriers were decreased after applying the electric field. The results suggest that the electric field can be used to realize a fast charging process of rechargeable ion batteries.

Acknowledgement:

This work was financially supported by the National Natural Science Foundation of China (11474047). Funding support from the UoA and CAPEX from Northumbria University at Newcastle, and Royal academy of Engineering UK-Research Exchange with China and India is acknowledged. This work was carried out at National Supercomputer Center in Tianjin, and the calculations were performed on TianHe-1(A).

References:

[1] X. Bian, Q. Fu, C. Qiu, X. Bie, F. Du, Y. Wang, Y. Zhang, H. Qiu, G. Chen, Y. Wei, Materials Chemistry and Physics, 156 (2015) 69-75.

[2] W. He, X. Li, J. Chen, F. Peng, R. Zhang, Y. Liu, Z. Xiao, Materials Chemistry and Physics, 155 (2015) 9-16.

[3] B.-M. Hwang, S.-J. Kim, Y.-W. Lee, H.-C. Park, D.-M. Kim, K.-W. Park, Materials Chemistry and Physics, 158 (2015) 138-143.

[4] P.R. Ilango, T. Subburaj, K. Prasanna, Y.N. Jo, C.W. Lee, Materials Chemistry and Physics, 158 (2015) 45-51.

[5] J.K. EunJoo Yoo, Eiji Hosono, Hao-shen Zhou, Tetsuichi Kudo, Nano Lett, 8 (2008) 2277-2282.

[6] N. Amdouni, H. Zarrouk, F. Soulette, C. Julien, Materials Chemistry and Physics, 80 (2003) 205-214.

[7] Y.N. Ko, J.H. Kim, Y.J. Hong, Y.C. Kang, Materials Chemistry and Physics, 131 (2011) 292-296.

[8] W. Quan, Z. Tang, J. Zhang, Z. Zhang, Materials Chemistry and Physics, 147 (2014) 333-338.

[9] G. Wang, X. Shen, J. Yao, J. Park, Carbon, 47 (2009) 2049-2053.

[10] D. Wang, R. Kou, D. Choi, Z. Yang, Z. Nie, J. Li, L.V. Saraf, D. Hu, J. Zhang, G.L. Graff, J. Liu, M.A. Pope, I.A. Aksay, ACS Nano, 4 (2010) 1587-1595.

[11] D. Nasr Esfahani, O. Leenaerts, H. Sahin, B. Partoens, F.M. Peeters, The Journal of Physical Chemistry C, 119 (2015) 10602-10609.

[12] Z. Wang, Q. Su, H. Deng, Physical Chemistry Chemical Physics, 15 (2013) 8705-8709.

[13] H. Pan, Journal of Materials Chemistry A, 3 (2015) 21486-21493.

[14] K.K. Ghuman, S. Yadav, C.V. Singh, The Journal of Physical Chemistry C, 119 (2015) 6518-6529.

[15] D. Voiry, M. Salehi, R. Silva, T. Fujita, M. Chen, T. Asefa, V.B. Shenoy, G. Eda, M. Chhowalla, Nano Lett., 13 (2013) 6222-6227.

[16] X. Wang, X. Shen, Z. Wang, R. Yu, L. Chen, ACS Nano, 8 (2014) 11394-11400.

[17] L. Wang, Z. Xu, W. Wang, X. Bai, J. Am. Chem. Soc., 136 (2014) 6693-6697.

[18] Y. Cheng, A. Nie, Q. Zhang, L.-Y. Gan, R. Shahbazian-Yassar, U. Schwingenschlogl, ACS Nano, 8 (2014) 11447-11453.

[19] B. Radisavljevic, A. Radenovic, J. Brivio, V. Giacometti, A. Kis, Nat. Nanotechnol., 6 (2011) 147-150.

[20] C. Lee, H. Yan, L.E. Brus, T.F. Heinz, J. Hone, S. Ryu, ACS Nano, 4 (2010) 2695-2700.

[21] J.W. Seo, Y.W. Jun, S.W. Park, H. Nah, T. Moon, B. Park, J.G. Kim, Y.J. Kim, J. Cheon, Angew. Chem.-Int. Edit., 46 (2007) 8828-8831.

[22] S. Balendhran, J.Z. Ou, M. Bhaskaran, S. Sriram, S. Ippolito, Z. Vasic, E. Kats, S. Bhargava, S. Zhuiykov, K. Kalantar-zadeh, Nanoscale, 4 (2012) 461-466.

[23] J.V. Lauritsen, J. Kibsgaard, S. Helveg, H. Topsoe, B.S. Clausen, E. Laegsgaard, F. Besenbacher, Nat. Nanotechnol., 2 (2007) 53-58.

[24] F.Y. Xiong, Z.Y. Cai, L.B. Qu, P.F. Zhang, Z.F. Yuan, O.K. Asare, W.W. Xu, C. Lin, L.Q. Mai, ACS Appl. Mater. Interfaces, 7 (2015) 12625-12630.

[25] X.Y. Yu, H. Hu, Y.W. Wang, H.Y. Chen, X.W. Lou, Angew. Chem.-Int. Edit., 54 (2015) 7395-7398.

[26] Y.C. Liu, Y.P. Zhao, L.F. Jiao, J. Chen, Journal Of Materials Chemistry A, 2 (2014) 13109-13115.

[27] Y.H. Lu, J.B. Goodenough, J. Mater. Chem., 21 (2011) 10113-10117.

[28] T. Ichitsubo, T. Adachi, S. Yagi, T. Doi, J. Mater. Chem., 21 (2011) 11764-11772.

[29] Y. Liang, H.D. Yoo, Y. Li, J. Shuai, H.A. Calderon, F.C. Robles Hernandez, L.C. Grabow, Y. Yao, Nano Lett., 15 (2015) 2194-2202.

[30] Y. Liu, L. Jiao, Q. Wu, Y. Zhao, K. Cao, H. Liu, Y. Wang, H. Yuan, Nanoscale, 5 (2013) 9562-9567.

[31] L. David, R. Bhandavat, G. Singh, ACS Nano, 8 (2014) 1759-1770.

[32] S. Yang, D. Li, T. Zhang, Z. Tao, J. Chen, The Journal of Physical Chemistry C, 116 (2012) 1307-1312.

[33] Y. Liang, R. Feng, S. Yang, H. Ma, J. Liang, J. Chen, Advanced Materials, 23 (2011) 640-643.

[34] M. Mortazavi, C. Wang, J. Deng, V.B. Shenoy, N.V. Medhekar, Journal of Power Sources, 268 (2014) 279-286.

[35] W.-H. Ryu, J.-W. Jung, K. Park, S.-J. Kim, I.-D. Kim, Nanoscale, 6 (2014) 10975-10981.

[36] C. Zhu, X. Mu, P.A. van Aken, J. Maier, Y. Yu, Advanced Energy Materials, 5 (2015) n/a-n/a.

[37] D. Datta, J. Li, N. Koratkar, V.B. Shenoy, Carbon, 80 (2014) 305-310.

[38] D. Nasr Esfahani, O. Leenaerts, H. Sahin, B. Partoens, F.M. Peeters, The Journal of Physical Chemistry C, 119 (2015) 10602-10609.

[39] Y. Li, D. Wu, Z. Zhou, C.R. Cabrera, Z. Chen, The Journal of Physical Chemistry Letters, 3 (2012) 2221-2227.

[40] L.-p. Feng, J. Su, S. Chen, Z.-t. Liu, Materials Chemistry and Physics, 148 (2014) 5-9.

[41] Z. Wang, Q. Su, G.Q. Yin, J. Shi, H. Deng, J. Guan, M.P. Wu, Y.L. Zhou, H.L. Lou, Y.Q. Fu, Materials Chemistry and Physics, 147 (2014) 1068-1073.

[42] X. Sun, Z. Wang, Y.Q. Fu, Scientific Reports, 5 (2015) 18712.

[43] W. Shi, S. Wu, Z. Wang, Physica E: Low-dimensional Systems and Nanostructures, 81 (2016) 192-195.

[44] J. Qi, X. Li, X. Qian, J. Feng, Applied Physics Letters, 102 (2013) 173112.

[45] L. Kou, C. Tang, Y. Zhang, T. Heine, C. Chen, T. Frauenheim, The Journal of Physical Chemistry Letters, 3 (2012) 2934-2941.

[46] Q. Yue, Z. Shao, S. Chang, J. Li, Nanoscale Research Letters, 8 (2013) 1-7.

[47] J.M. Soler, E. Artacho, J.D. Gale, A. Garcia, J. Junquera, P. Ordejon, D. Sanchez-Portal, J Phys-Condens Mat, 14 (2002) 2745-2779.

[48] N. Troullier, J.L. Martins, Physical Review B, 43 (1991) 1993-2006.

[49] J.P. Perdew, W. Yue, Physical Review B, 33 (1986) 8800-8802.

[50] J.D. Pack, H.J. Monkhorst, Physical Review B, 16 (1977) 1748-1749.

[51] J. Neugebauer, M. Scheffler, Physical Review B, 46 (1992) 16067-16080.

[52] P. Rastogi, S. Kumar, S. Bhowmick, A. Agarwal, Y.S. Chauhan, The Journal of Physical Chemistry C, 118 (2014) 30309-30314.

[53] H.J. Chen, J. Huang, X.L. Lei, M.S. Wu, G. Liu, C.Y. Ouyang, B. Xu, International Journal Of Electrochemical Science, 8 (2013) 2196-2203.

[54] A.O. Pereira, C.R. Miranda, The Journal of Physical Chemistry C, 119 (2015) 4302-4311.

[55] Y.G. Guo, J.S. Hu, L.J. Wan, Adv. Mater., 20 (2008) 2878-2887.

[56] G. Henkelman, G. Jóhannesson, H. Jónsson, Methods for Finding Saddle Points and Minimum Energy Paths, in: S.D. Schwartz (Ed.) Theoretical Methods in Condensed Phase Chemistry, Springer Netherlands, Dordrecht, 2002, pp. 269-302.

[57] G. Henkelman, B.P. Uberuaga, H. Jonsson, J. Chem. Phys., 113 (2000) 9901-9904.

[58] G.H. Vineyard, Journal of Physics and Chemistry of Solids, 3 (1957) 121-127.

[59] J. Wong, S. Yadav, J. Tam, C. Veer Singh, Journal of Applied Physics, 115 (2014) 224301.

[60] J. Carrasco, The Journal of Physical Chemistry C, 118 (2014) 19599-19607.

[61] M. Dion, H. Rydberg, E. Schröder, D.C. Langreth, B.I. Lundqvist, Physical Review Letters, 92 (2004) 246401.

[62] H. Yildirim, A. Kinaci, Z.-J. Zhao, M.K.Y. Chan, J.P. Greeley, ACS Appl. Mater. Interfaces, 6 (2014) 21141-21150.

[63] X. Fan, W.T. Zheng, J.-L. Kuo, ACS Appl. Mater. Interfaces, 4 (2012) 2432-2438.

[64] L.-J. Zhou, Z.F. Hou, L.-M. Wu, The Journal of Physical Chemistry C, 116 (2012) 21780-21787.

[65] L.-J. Zhou, Z.F. Hou, L.-M. Wu, Y.-F. Zhang, The Journal of Physical Chemistry C, 118 (2014) 28055-28062.

[66] J. Setiadi, M.D. Arnold, M.J. Ford, ACS Appl. Mater. Interfaces, 5 (2013) 10690-10695.

[67] X. Sun, Z. Wang, Z. Li, Y.Q. Fu, Scientific Reports, 6 (2016) 26666.

Lists of figures captions:

Figure 1 (a) Top and (b) side views of MoS_2 monolayer supercell with atoms. Electric field was applied with its orientation perpendicular to the monolayer.

Figure 2 Adsorption energies as a function of applied electric field.

Figure 3 (a) Diffusion path of atom from one stable site (T) to another one through metal-stable site (H). Diffusion energy curves for (b) Li, (c) Mg and (d) Al atoms from one stable position to a neighbor one with and without electric field.

Figure 4 Diffusion barriers as a function of applied electric field. The diffusion barriers decreased with the electric field.

Figure 5 (a) Diffusion path and (b) diffusion energy curves of Li atom from T site H site with larger Li concentration.

Figure 6 A prototypes of rechargeable ion batteries with fast charging process.

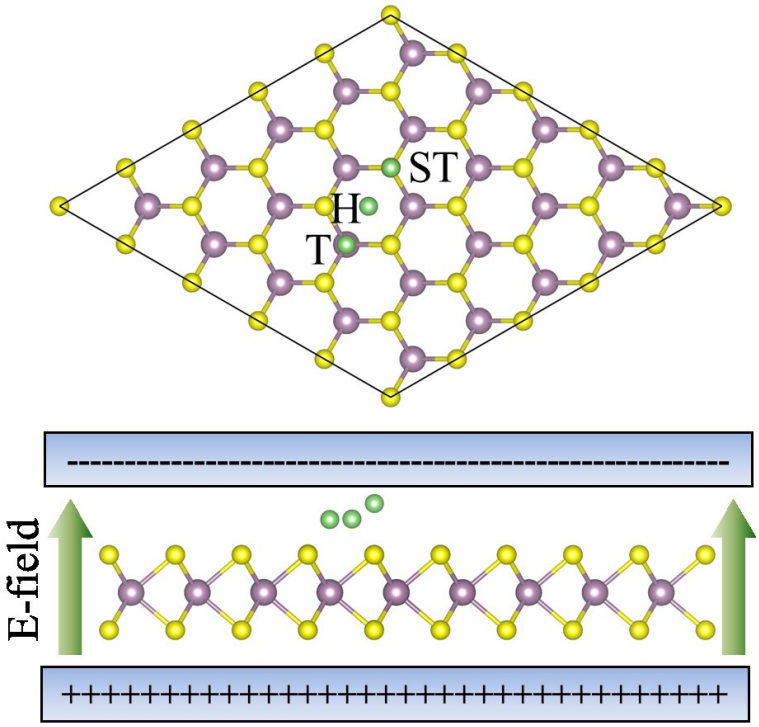

W.W. Shi et al. Figure 1

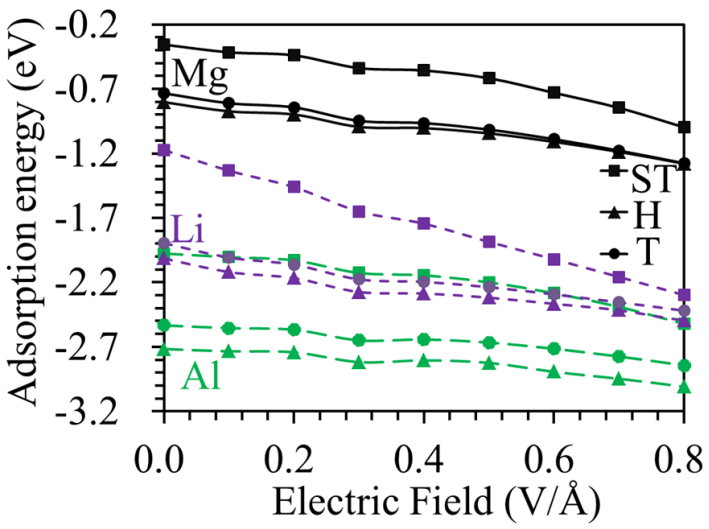

W.W. Shi et al. Figure 2

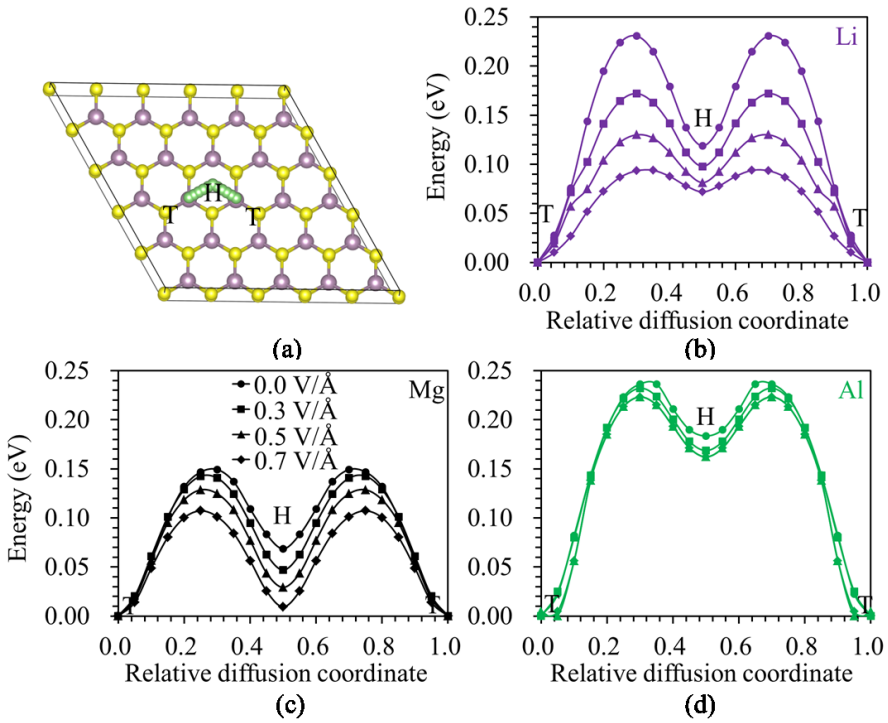

W.W. Shi et al. Figure 3

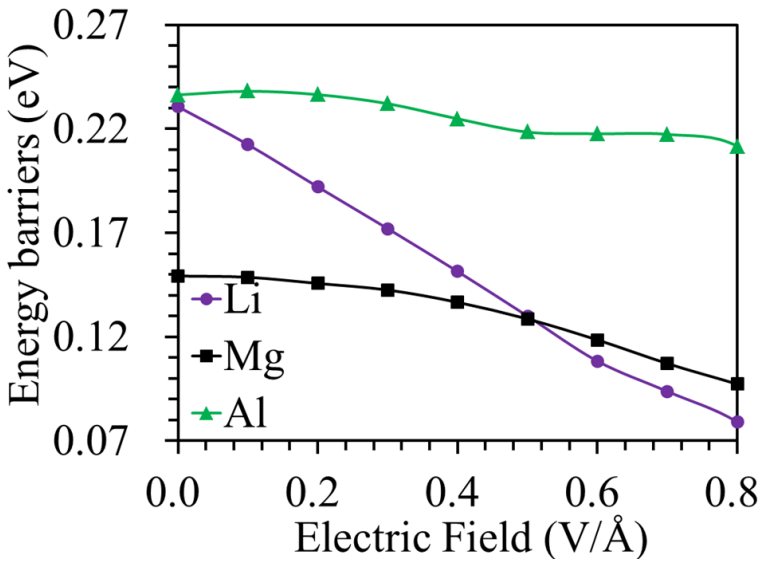

W.W. Shi et al. Figure 4

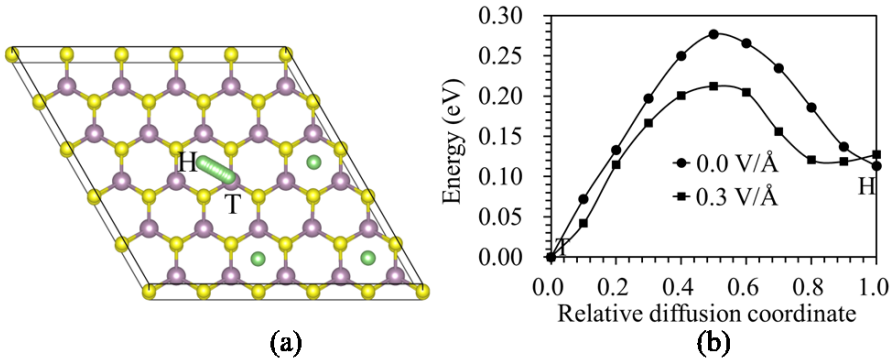

W.W. Shi et al. Figure 5

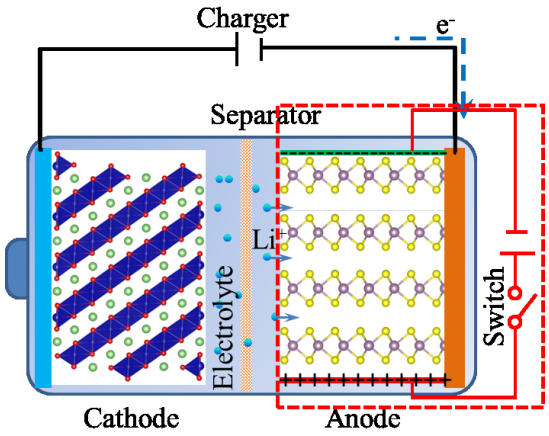

W.W. Shi et al. Figure 6